

Single-junction solar cells based on *p-i-n* GaAsSbN heterostructures grown by liquid phase epitaxy

Malina Milanova^a, Vesselin Donchev^{b*}, Kieran Cheetham^c, Zhongming Cao^d, Ian Sandall^d, Giacomo M. Piana^e, Oliver S. Hutter^f, Ken Durose^c, Asim Mumtaz^c

^a Central Laboratory of Applied Physics, Bulgarian Academy of Sciences, 61, St. Petersburg blvd., 4000 Plovdiv, Bulgaria

^b Faculty of Physics, Sofia University, blvd. James Bourchier, 5, 1164 Sofia, Bulgaria

^c Department of Physics, Stephenson Institute for Renewable Energy, University of Liverpool, L69 7ZF, U.K.

^d Department of Electrical Engineering and Electronics, University of Liverpool, L69 3GJ, U.K.

^e Department of Physics and Astronomy, University of Southampton, University Road, Southampton SO17 1BJ, U.K.

^f Department of Mathematics, Physics and Electrical Engineering, Northumbria University, Newcastle upon Tyne NE1 8ST, UK.

ABSTRACT

In this paper we present single heterojunction *p-i-n* GaAsSbN/GaAs solar cells grown by low-temperature liquid-phase epitaxy (LPE) – this is of interest as a component of multi-junction solar cell devices. The quaternary absorber layer was characterized by low excitation power photoluminescence to give the temperature dependence of the band gap. This conformed to

*Corresponding author.

E-mail address: vtd@phys.uni-sofia.bg (V. Donchev).

the Varshni function at low temperatures to within 10 meV, indicating relatively small alloy potential fluctuations. The absorption properties and the transport of the photogenerated carriers in the heterostructures was investigated using surface photovoltage method. A power conversion efficiency of 4.15 % (AM1.5, 1000 W.m⁻²) was measured for p-i-n GaAsSbN/GaAs solar cells, which is comparable to the efficiency of MOCVD grown devices of this type. This is promising for the first report of LPE grown GaAsSbN/GaAs solar cells since the current record efficiency for the cells based on these compounds grown by MBE stands just at 6 %. The long-wavelength photosensitivity of the cells determined from external quantum efficiency and surface photovoltage measurements was shown to be extended to 1040 nm.

Keywords

GaAsSbN, liquid phase epitaxy, p-i-n heterostructures, solar cells, photovoltaic

1. Introduction

There has been great interest in dilute nitride III-V-N materials during the last two decades, driven in part by their potential application in multijunction solar cells (Friedman et al., 1998; Geisz et al., 2018; Harris, 2005; Isoaho et al., 2019; Johnston et al., 2005; Kurtz et al., 2002; Miyashita et al., 2013, 2012; Ptak et al., 2009, 2005) which are expected to outperform single junction devices. A conversion efficiency of 46.1 % has been reported for four-junction solar cells under concentrated light, using wafer bonding to combine 2 two-junction solar cells grown on InP and GaAs substrates (Dimroth et al., 2016). The efficiency record is currently held by NREL for a six-junction inverted metamorphic concentrator solar cell which achieved 47.1 % (Geisz et al., 2018). The bandgap combination of the subcells is a key factor for further improvements in the overall cell efficiency. Presently multi-junction solar

cell performance is limited by the performance of the subcells which need to be chosen for their bandgaps and also need to be grown with appropriate crystal quality. Dilute nitride alloys such as InGaAsN or GaAsSbN can provide adjustable bandgaps between 1.2 and 0.8 eV while remaining lattice-matched to GaAs or Ge substrates. Hence the development of these materials is of great significance for high-efficiency multijunction solar cells, where they can be used to collect the low-energy photons. However, the device performance has not reached expectations, due to the low radiative efficiencies and low minority carrier diffusion lengths (Johnston et al., 2005; Kurtz et al., 2002). The issue of poor minority carrier diffusion length has been partially tackled by increasing the depletion region width by the use of undoped layers to increase the current (Miyashita et al., 2012; Ptak et al., 2005). However, the trap-assisted recombination dark current increases with the width of the depletion region, which leads to the lowering of the open-circuit voltage.

It is therefore essential to improve the properties of dilute nitride compounds. There has been significant progress in the development of InGaAsN materials. InGaAsN solar cells grown by metalorganic chemical vapour deposition (MOCVD). A device based on a double-heterostructure single-junction (and using an anti-reflection coating) has achieved 13.2 % efficiency as reported by Kim *et al.* (Kim et al., 2015). The Solar Junction Corporation reported the highest efficiency monolithic triple-junction solar cells of 43.5 % under concentrated light for using InGaAsN instead of Ge as the lowest subcell (Wiemer et al., 2011).

Another dilute nitride material suitable for solar cell applications as an alternative to InGaAsN is GaAsSbN. It offers the possibility for independent tuning of the conduction and valence bands. While the bandgap of dilute nitrides is primarily reduced by lowering the conduction band minimum, the bandgap of antimonides is reduced by raising the valence band maximum energy. Both of these mechanisms are explained through the band anti-

crossing model. The incorporation of both Sb and N atoms into the crystal lattice enables lattice matching with GaAs or Ge. In addition, their incorporation also causes a large concentration of localized states which results in changed electronic and optical properties, and lower device performance, due to reduced carrier collection. Despite the beneficial features of this material it has not been as widely studied as InGaAsN, although interest in GaAsSbN has risen over the last few years (Bian et al., 2004; Gonzalo et al., 2019; T. W. Kim et al., 2014; Kim, Tae Wan et al., 2014; Lin et al., 2013; Milanova et al., 2019; Tan et al., 2011; Thomas et al., 2015; Yurong et al., 2017). Recent solar cells based on GaAsSbN have demonstrated efficiencies of 4 % for a nonoptimized single-junction solar cell structure, without anti-reflection coating grown by MOCVD (Kim, Tae Wan et al., 2014) and 6 % for molecular beam epitaxy (MBE) grown structures (Thomas et al., 2015).

In this paper, we present the results of single-heterojunction p-i-n GaAsSbN solar cells grown by low-cost liquid phase epitaxy (LPE) method. To the best of our knowledge, no other groups have reported on LPE grown GaAsSbN/GaAs heterostructures. Temperature-dependent photoluminescence (PL) spectra at a low excitation power of 0.5 mW have been used to identify the in-gap localized states, which increase the dark current of the cells. In the first device trials for LPE GaAsSbN/GaAs devices, efficiencies of 4.15 % were achieved under AM1.5 conditions on areas of 3.5 x 3.5 mm².

2. Experimental Methods

The schematic structure of the single-junction solar cell investigated in this study is shown in Fig. 1. It employs a *p-i-n* structure based on compensated GaAsSbN layers grown via LPE. The epitaxial structures were grown in a horizontal LPE reactor using the “piston boat” technique. The starting materials were Ga and Sb metal-solvents of 6N purity, and polycrystalline GaAs and GaN powder used as sources for As and N, respectively. The

elements chosen as dopants were Te for n-type doping and Mg for p-type doping. The epitaxial structure was grown in the temperature interval 640-546 °C at a cooling rate 0.8°C/min. Dilute nitride i-GaAsSbN layer was grown from a 7°C supercooled mixed Ga + 5 at. % Sb solution in the temperature range 558 -550 °C. The GaAs capping and AlGaAs “window” layers were grown in the temperature intervals 550-548 °C and 548 -546°C, respectively. The Sb content in the GaAs_{1-x-y}Sb_xN_y layers was measured in several points on a cross-section by energy-dispersive X-ray spectroscopy (EDX). The average value of *x* was determined to be 6.7 % and it is confirmed by X-ray photoelectron spectroscopy (XPS) measurements. The presence of 0.1% nitrogen in the studied samples was determined by XPS measurements using excitation with Mg K α radiation. The lattice mismatch between the LPE grown GaAsSbN layers and the GaAs substrate is about 0.48 %, as was determined from X-ray diffraction (004) curves. The details on structural characterization are presented in Ref. (Milanova et al., 2019)

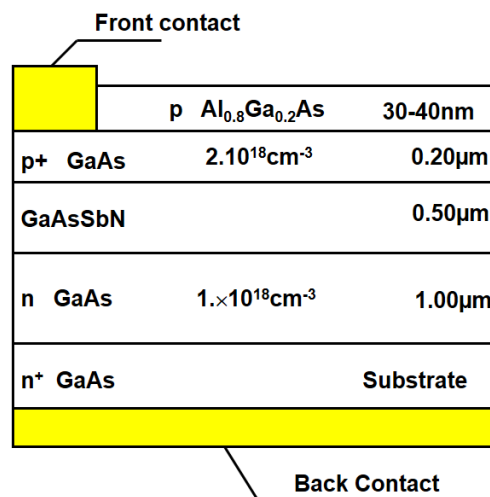


Fig. 1. Schematic structure of a single-junction *p-i-n* solar cell based on compensated GaAsSbN heterostructure grown by LPE.

Samples were processed into $3.5 \times 3.5 \text{ mm}^2$ photovoltaic mesa diodes comprising of a 3 mm diameter optical window using standard mask lithography. Firstly, a common back *n*-contact was formed via thermal evaporation of an InGe/Au layer, which was subsequently annealed at 400°C for 1 minute. Following this, top Ohmic contacts were defined via lithography consisting of $10 \text{ }\mu\text{m}$ wide stripes, separated by $90 \text{ }\mu\text{m}$, across the optical window to ensure homogenous current injection. The contacts were deposited via thermal evaporation, which consisted of Au/Zn/Au layers, and subsequently followed by a 380°C anneal for 1 minute. Prior to the contact deposition the top $\text{Al}_{0.8}\text{Ga}_{0.2}\text{As}$ layer was selectively etched using hydrogen peroxide and citric acid solution. The mesas were then etched using phosphoric acid, hydrogen peroxide and de-ionized water etchant. They were etched to a sufficient depth to ensure electrical isolation between adjacent devices.

Temperature dependent PL spectra were measured in the temperature range between 10 and 150 K in order to investigate the optical properties of the grown structures. The excitation was obtained with a laser light having an energy density of 100 nJ/cm^2 (80 MHz repetition rate and $550 \text{ }\mu\text{W}$ laser power) and wavelength of 680 nm provided by supercontinuum white laser (Fianium WhiteLase) monochromated with a tunable bandpass transmission filter (Fianium SuperChrome). The light spot diameter on the sample surface was $130 \text{ }\mu\text{m}$. The sample was mounted in a closed-loop He cryostat and its temperature was controlled through an Oxford Instruments ITC503 unit. The PL was collected and recorded by a fibre-coupled spectrometer (BWSpec Glacier X). Surface photovoltage (SPV) spectroscopy in metal-insulator-semiconductor (MIS) operation mode was undertaken. This technique was applied to study the optical absorption of the structures using the set-up and the measurement procedure as described elsewhere (Donchev, 2019).

J-V measurements were undertaken using a calibrated TS Space Systems solar simulator with an AM1.5 spectrum at 1000 Wm^{-2} . The external quantum efficiency (EQE) measurements were performed using a Bentham PVE 300 system in the dark, i.e. without white light bias. A total of 8 different solar cell variants were produced, each sample having approximately 9 complete cells.

3. Results and Discussion:

3.1 Photoluminescence Characterization

The temperature-dependent PL spectra of a solar cell epitaxial structure in the range 11 K - 300 K measured under low excitation intensity ($\sim 0.5 \text{ W/cm}^2$) are depicted in Fig. 2. The peak with high intensity comes from the p+ GaAs layer and the weak peak red-shifted to GaAs comes from GaAsSbN layer of the structure.

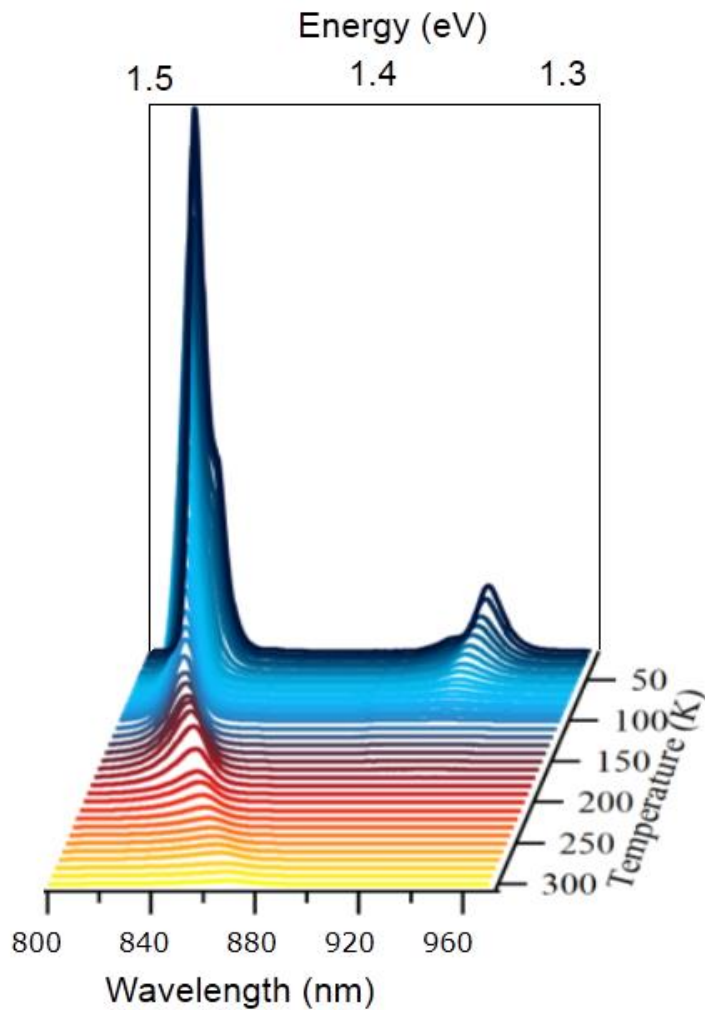


Fig. 2. Temperature dependent PL spectra of a GaAsSbN/GaAs solar cell structure in the range 15-300 K with step intervals of 10 K.

Fig. 3 presents the normalized PL peaks of the GaAsSbN layer in the structure measured in the range (11 – 150 K). The PL peak energy evolution presents an anomalous, nearly S-shaped temperature behaviour. It is seen that there is a blue shift of the PL emission energy as the temperature is increased from 10 to about 60-70 K. With further increase of the temperature (beyond 70 K) the PL peak exhibits a red shift. This type of behaviour is a well-known characteristic of carrier localization effects associated with band-tail states (Gao et al., 2016; Lai et al., 2006; Lourenço et al., 2007) which are known to depend on the degree of disorder of the compound. In the quaternary GaAsSbN compounds the incorporation of N and

Sb into the crystal lattice locally modifies the conduction and valence bands respectively, thus creating localized states and potential fluctuations. The blue-shift of the emission at low temperatures indicates that as the temperature increases the excitons gain sufficient thermal energy to transfer to higher-energy localized levels, thus increasing the emission energy. As the temperature increases further (above 70 K) the higher energy localized states are gradually saturated, the excitons become almost delocalized and the PL peak energy decreases as a function of temperature due to reduction in the bandgap.

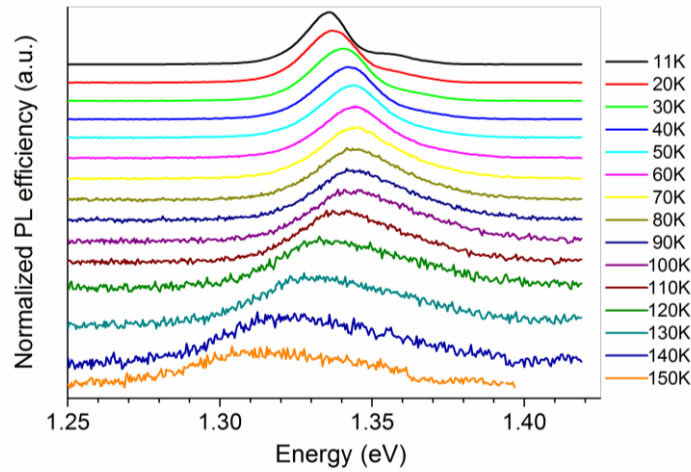


Fig. 3. Normalized PL spectra of GaAsSbN in a *p-i-n* solar cell structure measured from 11K (top) to 150 K (bottom) with step intervals of 10 K under excitation power of 0.5 W/cm².

Fig. 4 illustrates the variations of the PL peak energies as a function of temperature for the *p*⁺-GaAs and the GaAsSbN layer in the structure. The PL peak energy for GaAs decreases monotonically with increasing temperature. Its temperature dependence is well fitted with Varshni's relation $E_g(T) = E_0 - aT^2/(T+b)$ using the parameters typical for GaAs (Blakemore, 1982), namely $E_0 = 1.519$ eV for the bandgap at $T = 0$ K, and $a = 5.4 \times 10^{-4}$ eV.K⁻¹, and $b = 204$ K as fitting parameters.

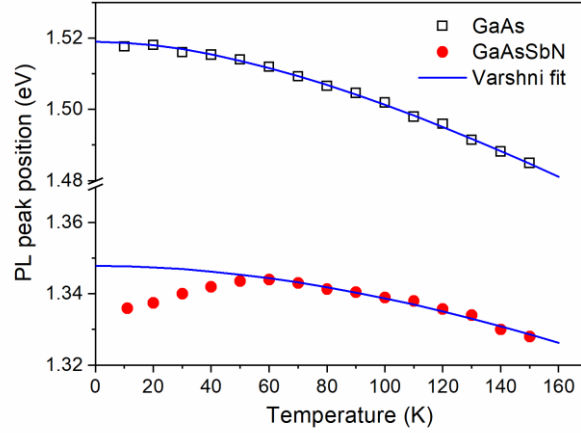


Fig. 4. Temperature dependence of the PL peak energy of GaAs (squares) and GaAsSbN (circles) in a *p-i-n* solar cell structure. Lines represent Varshni fits to the data.

The GaAsSbN peak exhibits the non-typical S-curve (blue-red) behaviour. The first red-shift is missing (see Fig.4), while the blue shift is only around 10 meV. This indicates that the potential fluctuations in these samples are relatively small and even at low temperature the excitons receive enough thermal energy to escape from the localized states and transfer to higher-energy localized states in the band-tail closer to the conduction band. The fit to the data above 60 K was obtained using Varshni's relation with the following fitting parameters: $E_0 = 1.348$ eV, $a = 6.41 \times 10^{-4}$ eV.K⁻¹ and $b = 600$ K. The blue shift of the PL peak energy observed in this work is compared to the blue shift measured in MBE grown GaAsSbN/GaAs single quantum wells after annealing. It is nearly the same as the values reported in (Li et al., 2005) for *in-situ* annealed samples, while in other works (Lourenço et al., 2007; Nunna et al., 2007) larger values were observed. In our previous work (Milanova et al., 2020) the temperature-dependent PL spectra of the *p-i-n* structures were measured under higher excitation intensity (5 W/cm²) and no blue shift of the PL peak position was observed at low temperatures. In the whole temperature range 20 – 300 K, the PL peak energy showed a

monotonous decrease with increasing temperature and this behaviour was well fitted by an empirical Varshni relation (Milanova et al., 2020).

Fig. 5 shows the temperature dependence of the PL full widths at half maximum (FWHM) for p^+ GaAs and GaAsSbN layers. The FWHM values increase monotonically with temperature from 7.3 meV at 11 K to 15.2 meV at 150 K for GaAs layer. The FWHM for GaAsSbN is 11.7 meV at 11 K and increases slightly from 14.5 meV to 18 meV in the temperature range 20 - 60 K where the emission is dominated by localized excitons. FWHM values increase more rapidly with increasing temperature above 60 K where the emission is dominated by delocalized excitons.

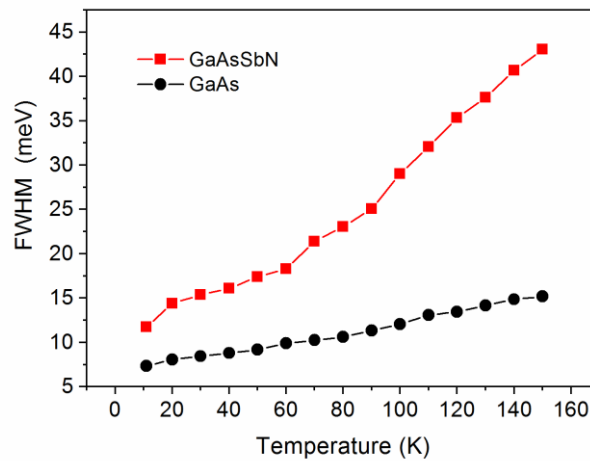


Fig. 5. Temperature dependence of the FWHM of the PL peak of GaAs (squares) and GaAsSbN (circles) in a p-i-n solar cell structure.

3.2. Surface photovoltage characterization

SPV spectroscopy has seldom been used to study dilute nitride materials, e.g. the optical absorption (Bansal et al., 2006) and the band offset (Galluppi et al., 2005) in InGaAsN/GaAs single quantum wells and the E_- and E_+ transitions in GaNAs layers (Kudrawiec et al.,

2014). However, no other groups have reported on SPV investigations of GaAsSbN dilute nitride materials. We apply this method to study the optical absorption and photocarrier transport in the investigated structures. It is well known that in MIS operation mode the SPV amplitude spectrum emulates the optical absorption spectrum (Kronik and Shapira, 1999), while the SPV phase spectrum carries information about the direction of the energy band bending and therefore about the direction of the photocarrier movement (Donchev, 2019). The SPV measurements were performed at room temperature with a light modulation frequency of 94 Hz. The scanning was from high to low wavelengths, keeping the photon flux constant at each wavelength.

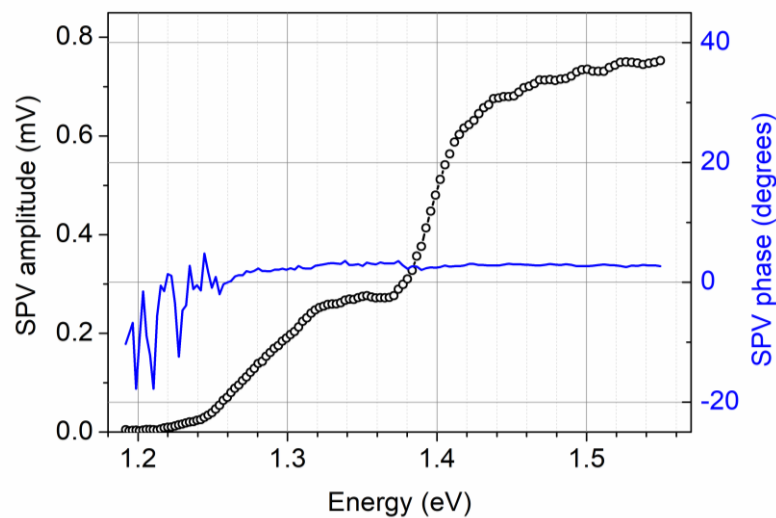


Fig. 6. Surface photovoltage amplitude (symbols) and phase (line) spectra of a *p-i-n* solar cell based on compensated GaAsSbN measured at room temperature.

Fig. 6 presents the SPV amplitude and phase spectra of a *p-i-n* single-junction solar cell structure based on compensated GaAsSbN. The amplitude spectrum reveals a step in the range of 1.24 – 1.38 eV and another one for energies above 1.38 eV. The former originates

from the absorption in the GaAsSbN layer and the latter from absorption in the GaAs layers. We emphasize that the signals from GaAsSbN and GaAs are comparable in magnitude, which attests for good quality of the dilute nitride layer. The absorption edge of GaAsSbN from SPV was confirmed by a Tauc plot as being 1.26 eV. Considering its thickness (0.5 μm) and Hall carrier concentration ($\sim 10^{15} \text{ cm}^{-3}$ (Milanova et al., 2020)) the GaAsSbN layer is fully depleted and the photogenerated electrons are swept towards the n -GaAs layer, while the holes – toward the p^+ -GaAs layer thus giving rise to photovoltage. The direction of the carrier drift is evidenced by the SPV phase values, which are close to zero degrees in agreement with the upward energy bands bending (in the direction towards the surface) in the p - i - n structure (Donchev, 2019).

3.3 Photovoltaic characterization: J-V and EQE characteristics

A typical J-V curve for the GaAsSbN p - i - n solar cell measured at AM1.5 conditions is presented in Fig. 7a. Fig. 7b shows the corresponding J-V curve measured in the dark. Photovoltaic parameters measured on several devices in this work are given in Table 1. The best solar cell shows an efficiency of 4.15 %, an open-circuit voltage $V_{oc} = 0.44 \text{ V}$, short-circuit current $J_{sc} = 17.31 \text{ mAcm}^{-2}$ and fill factor $FF = 54.5 \%$. The series resistance is $R_{series} = 5.73 \text{ }\Omega\text{cm}^2$ and shunt resistance is $R_{shunt} = 478 \text{ }\Omega\text{cm}^2$. This is comparable to the efficiency reported for single-junction 1.25 eV GaAsSbN solar cells with 600 nm thickness of the GaAsSbN base layer grown by MOCVD (Kim, Tae Wan et al., 2014). A higher efficiency of about 6 % has been achieved for 1.15 eV MBE grown GaAsSbN solar cells (Thomas et al., 2015). In both cases, a rapid thermal annealing (RTA) at 800°C of the solar cells was performed, which significantly increased the open-circuit voltage values to 0.5 – 0.6 V due to the decrease in the density of the localized states. However, typical values of V_{oc} measured in our cells based on as-grown LPE structures without RTA are in the range 0.40 – 0.44 V.

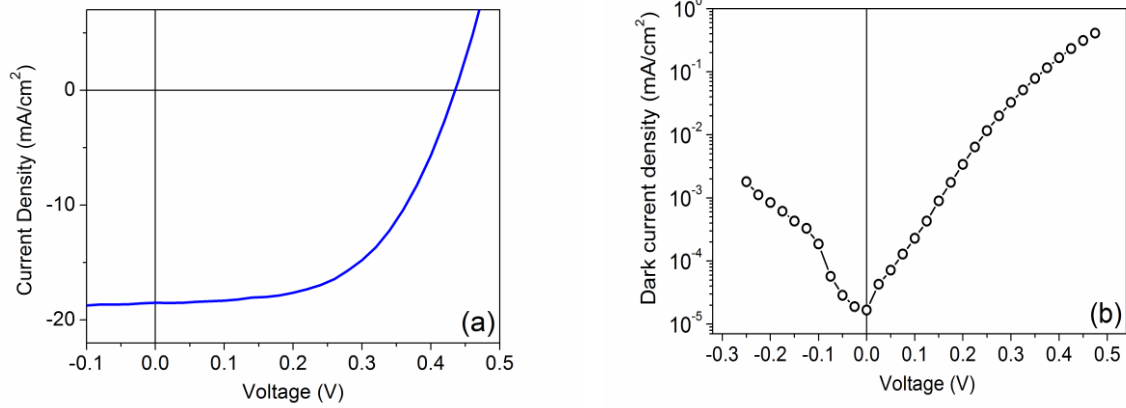


Fig. 7. J-V curves of a GaAsSbN *p-i-n* solar cell measured at AM1.5 conditions (a) and in the dark (b).

Table. 1. PV parameters of several devices measured in this work

Sample	Efficiency	V_{oc} [V]	I_{sc} [mA/cm ²]	FF [%]
E407	4.00	0.43	17.58	53
	4.02	0.44	17.26	53
	4.07	0.43	17.85	53
E409	4.10	0.44	17.27	53.90
	4.09	0.44	16.92	55.00
	4.15	0.44	17.31	54.50
	4.06	0.44	17.23	53.50
E410	4.10	0.43	18.7	51
	4.03	0.42	18.45	52
	3.87	0.41	18.16	52

Theoretically calculated V_{oc} values for the cells with 1.2 eV bandgap are about 0.8 V assuming that the charge transport is dominated mainly by diffusion of minority carriers.

However, even in the best cells, different recombination mechanisms are present which lower the maximum open-circuit voltages below the theoretical limits. It is known that the

incorporation even of a small quantity of nitrogen ($\sim 0.1\%$) into GaAs creates a high concentration of minority carriers traps which sufficiently increases the dark current. To identify the limiting factors of V_{oc} , we have determined the saturation dark current from the dark J-V measurements, which is dominated by trap-assisted recombination in the depletion region. The saturated dark current density J_0 of the cell obtained from the presented dark J-V characteristic is around 10^{-5} mA/cm². This value is about three orders of magnitude higher than those for the high-quality cells which is due to the carrier recombination via N-induced traps in the GaAsSbN layer. The increase in dark current is directly related to the decreased V_{oc} values of the solar cells. In addition, the lowering in V_{oc} values could be explained by a change in the position of the quasi-Fermi levels from the carrier traps, occurred by the incorporation of N and Sb into the crystal lattice (Kurtz et al., 2005).

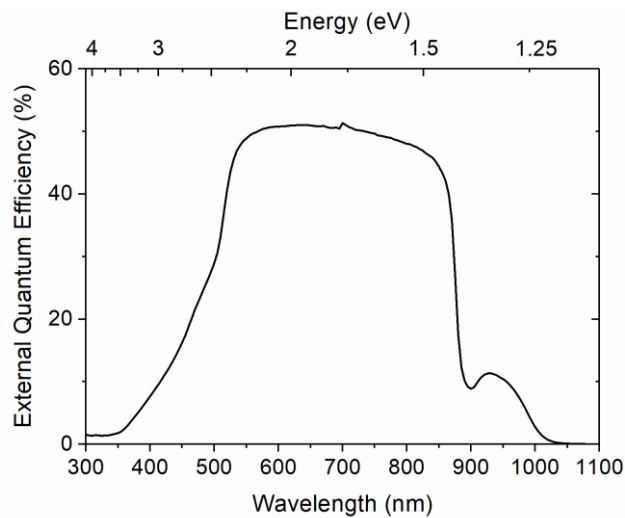


Fig.8. EQE of a GaAsSbN *p-i-n* solar cell.

An example of a corresponding EQE graph is given in Fig. 8. EQE values of around 50 % were measured in the wavelength range 550 – 850 nm, which suggests that the upper p^+ -

GaAs emitter layer is of good quality despite being grown on GaAsSbN. A significant decrease of the EQE in the infrared part of the spectrum is due to the short minority carrier diffusion length in the dilute nitride layer because of the efficient recombination via localized defect levels. Nevertheless, the EQE extends to approximately 1040 nm (1.19 eV) with an inflexion point at 1.26 eV in agreement with the SPV results for the bandgap of GaAsSbN. A slight reduction in EQE is observed at approximately 900 nm (1.377 eV), which can be associated with the onset of the optical transitions in GaAs in accordance with the SPV spectrum. The short wavelength photosensitivity of the structure is determined by the composition and thickness of the AlGaAs layer.

4. Conclusions

Single junction solar cells based on a *p-i-n* GaAsSbN/GaAs structure grown via LPE were developed and studied. Mesa diodes measuring $3.5 \times 3.5 \text{ mm}^2$ with circular optical window 3 mm in diameter were fabricated using standard lithography and wet etch processing. *n*- and *p*- type Ohmic contacts based on InGe/Au and Au/Zn/Au were deposited via thermal evaporation on the back and the front surface of the cells. Temperature-dependent PL measurements at low excitation power of 0.5 mW show a slight blue shift of the GaAsSbN PL emission energy at low temperatures from 10 K to about 70 K, which led to the conclusion that the potential fluctuations are relatively small. SPV measurements provide information on the optical absorption and photocarrier transport in the investigated structures. The bandgap energy at room temperature of GaAsSbN determined from the optical absorption edge is 1.26 eV. Nearly the same IR photosensitivity behaviour was revealed from EQE measurements.

J-V curves were measured under standard test conditions (25°C, one sun AM1.5). A power conversion efficiency of 4.15 %, an open-circuit voltage of 0.44 V, short-circuit current of 17.31 mA/cm^2 and fill factor 54.5 % were obtained for the cells without anti-

reflection coatings and without the rapid thermal annealing that has achieved higher voltages for MOVPE and MBE materials. This is very promising result for the first LPE grown GaAsSbN/GaAs solar cells, especially given that these cells are non-optimized, and the record GaAsSbN/GaAs solar cell currently stands at just 6 % efficiency. Further improvements in materials quality and in device design are needed to ensure higher photovoltaic performance of these cells.

Declaration of competing interest

The authors declare that they have no known competing financial interests or personal relationships that could have appeared to influence the work reported in this paper.

Acknowledgements

This work was supported by the Cost Action MP1406 "Multiscale in modelling and validation for solar photovoltaics (MultiscaleSolar)" and the Bulgarian Ministry of Education and Science under the National Research Program E+: Low Carbon Energy for the Transport and Households (grant agreement D01-214/2018). A. Mumtaz acknowledges support from the EPSRC Centre for Doctoral Training in New & Sustainable Photovoltaics, EP/L01551X/1. Tim Veal is gratefully acknowledged for discussions and useful suggestions in the write up of this paper.

References

- Bansal, B., Kadir, A., Bhattacharya, A., Arora, B.M., Bhat, R., 2006. Alloy disorder effects on the room temperature optical properties of GaInNAs quantum wells. *Appl. Phys. Lett.* 89, 032110. <https://doi.org/10.1063/1.2227618>
- Bian, L.F., Jiang, D.S., Tan, P.H., Lu, S.L., Sun, B.Q., Li, L.H., Harmand, J.C., 2004.

- Photoluminescence characteristics of GaAsSbN/GaAs epilayers lattice-matched to GaAs substrates. *Solid State Commun.* 132, 707–711. <https://doi.org/10.1016/j.ssc.2004.09.016>
- Blakemore, J.S., 1982. Semiconducting and other major properties of gallium arsenide. *J. Appl. Phys.* 53, R123–R181. <https://doi.org/10.1063/1.331665>
- Dimroth, F., Tibbits, T.N.D., Niemeyer, M., Predan, F., Beutel, P., Karcher, C., Oliva, E., Siefert, G., Lackner, D., Fus-Kailuweit, P., Bett, A.W., Krause, R., Drazek, C., Guiot, E., Wasselin, J., Tauzin, A., Signamarcheix, T., 2016. Four-junction wafer-bonded concentrator solar cells. *IEEE J. Photovoltaics* 6, 343–349. <https://doi.org/10.1109/JPHOTOV.2015.2501729>
- Donchev, V., 2019. Surface photovoltage spectroscopy of semiconductor materials for optoelectronic applications Surface photovoltage spectroscopy of semiconductor materials for optoelectronic applications. *Mater. Res. Express* 6, 103001. <https://doi.org/10.1088/2053-1591/ab3bf>
- Friedman, D.J., Geisz, J.F., Kurtz, S.R., Olson, J.M., 1998. 1-eV solar cells with GaInNAs active layer. *J. Cryst. Growth* 195, 409–415. [https://doi.org/10.1016/S0022-0248\(98\)00561-2](https://doi.org/10.1016/S0022-0248(98)00561-2)
- Galluppi, M., Geelhaar, L., Riechert, H., Hetterich, M., Grau, A., Birner, S., Stolz, W., 2005. Bound-to-bound and bound-to-free transitions in surface photovoltage spectra: Determination of the band offsets for $\text{In}_x\text{Ga}_{1-x}\text{As}$ and $\text{In}_x\text{Ga}_{1-x}\text{As}_{1-y}\text{Ny}$ quantum wells. *Phys. Rev. B - Condens. Matter Mater. Phys.* 72, 155324. <https://doi.org/10.1103/PhysRevB.72.155324>
- Gao, X., Wei, Z., Zhao, F., Yang, Y., Chen, R., Fang, X., Tang, J., Fang, D., Wang, D., Li, R., Ge, X., Ma, X., Wang, X., 2016. Investigation of localized states in GaAsSb epilayers grown by molecular beam epitaxy. *Sci. Rep.* 6, 29112. <https://doi.org/10.1038/srep29112>
- Geisz, J.F., Steiner, M.A., Jain, N., Schulte, K.L., France, R.M., McMahon, W.E., Perl, E.E.,

- Friedman, D.J., 2018. Building a six-junction inverted metamorphic concentrator solar cell. *IEEE J. Photovoltaics* 8, 626–632.
<https://doi.org/10.1109/JPHOTOV.2017.2778567>
- Gonzalo, A., Stanojević, L., Utrilla, A.D., Reyes, D.F., Braza, V., Fuertes Marrón, D., Ben, T., González, D., Hierro, A., Guzman, A., Ulloa, J.M., 2019. Open circuit voltage recovery in GaAsSbN-based solar cells: Role of deep N-related radiative states. *Sol. Energy Mater. Sol. Cells* 200, 109949. <https://doi.org/10.1016/j.solmat.2019.109949>
- Harris, J.S., 2005. The opportunities, successes and challenges for GaInNAsSb. *J. Cryst. Growth* 278, 3–17. <https://doi.org/10.1016/j.jcrysgro.2004.12.050>
- Isoaho, R., Aho, A., Tukiainen, A., Aho, T., Raappana, M., Salminen, T., Reuna, J., Guina, M., 2019. Photovoltaic properties of low-bandgap (0.7–0.9 eV) lattice-matched GaInNAsSb solar junctions grown by molecular beam epitaxy on GaAs. *Sol. Energy Mater. Sol. Cells* 195, 198–203. <https://doi.org/10.1016/j.solmat.2019.02.030>
- Johnston, S.W., Kurtz, S.R., Friedman, D.J., Ptak, A.J., Ahrenkiel, R.K., Crandall, R.S., 2005. Observed trapping of minority-carrier electrons in p -type GaAsN during deep-level transient spectroscopy measurement. *Appl. Phys. Lett.* 86, 1–3.
<https://doi.org/10.1063/1.1865328>
- Kim, T., Mawst, L.J., Kim, Y., Kim, K., Lee, J., Kuech, T.F., 2015. 13.2% efficiency double-hetero structure single-junction InGaAsN solar cells grown by MOVPE. *J. Vac. Sci. Technol. A Vacuum, Surfaces, Film.* 33, 021205. <https://doi.org/10.1116/1.4906511>
- Kim, T. W., Forghani, K., Mawst, L.J., Kuech, T.F., Lalumondiere, S.D., Sin, Y., Lotshaw, W.T., Moss, S.C., 2014. Properties of “bulk” GaAsSbN/GaAs for multi-junction solar cell application: Reduction of carbon background concentration. *J. Cryst. Growth* 393, 70–74. <https://doi.org/10.1016/j.jcrysgro.2013.10.034>
- Kim, Tae Wan, Kim, Y., Kim, K., Lee, J.J., Kuech, T., Mawst, L.J., 2014. 1.25-eV

- GaAsSbN/Ge double-junction solar cell grown by metalorganic vapor phase epitaxy for high efficiency multijunction solar cell application. *IEEE J. Photovoltaics* 4, 981–985.
<https://doi.org/10.1109/JPHOTOV.2014.2308728>
- Kronik, L., Shapira, Y., 1999. Surface photovoltage phenomena: Theory, experiment, and applications. *Surf. Sci. Rep.* 37, 1–206. [https://doi.org/10.1016/S0167-5729\(99\)00002-3](https://doi.org/10.1016/S0167-5729(99)00002-3)
- Kudrawiec, R., Sitarek, P., Gladysiewicz, M., Misiewicz, J., He, Y., Jin, Y., Vardar, G., Mintarov, A.M., Merz, J.L., Goldman, R.S., Yu, K.-M., Walukiewicz, W., 2014. Surface photovoltage and modulation spectroscopy of E⁻ and E⁺ transitions in GaNAs layers. *Thin Solid Films* 567, 101–104. <https://doi.org/10.1016/j.tsf.2014.07.052>
- Kurtz, S., Johnston, S., Branz, H.M., 2005. Capacitance-spectroscopy identification of a key defect in N-degraded GaInNAs solar cells. *Appl. Phys. Lett.* 86, 1–3.
<https://doi.org/10.1063/1.1884267>
- Kurtz, S.R., Klem, J.F., Allerman, A.A., Sieg, R.M., Seager, C.H., Jones, E.D., 2002. Minority carrier diffusion and defects in InGaAsN grown by molecular beam epitaxy. *Appl. Phys. Lett.* 80, 1379–1381. <https://doi.org/10.1063/1.1453480>
- Lai, F.-I., Kuo, S.Y., Wang, J.S., Kuo, H.C., Wang, S.C., Wang, H.S., Liang, C.T., Chen, Y.F., 2006. Effect of nitrogen contents on the temperature dependence of photoluminescence in InGaAsN/GaAs single quantum wells. *J. Vac. Sci. Technol. A* 24, 1223–1227. <https://doi.org/10.1116/1.2208996>
- Li, J., Iyer, S., Bharatan, S., Wu, L., Nunna, K., Collis, W., Bajaj, K.K., Matney, K., 2005. Annealing effects on the temperature dependence of photoluminescence characteristics of GaAsSbN single-quantum wells. *J. Appl. Phys.* 98, 013703.
<https://doi.org/10.1063/1.1931032>
- Lin, K.I., Lin, K.L., Wang, B.W., Lin, H.H., Hwang, J.S., 2013. Double-band anticrossing in GaAsSbN induced by nitrogen and antimony incorporation. *Appl. Phys. Express* 6,

121202. <https://doi.org/10.7567/APEX.6.121202>

Lourenço, S.A., Dias, I.F.L., Duarte, J.L., Laureto, E., Aquino, V.M., Harmand, J.C., 2007.

Temperature-dependent photoluminescence spectra of GaAsSb/AlGaAs and GaAsSbN/GaAs single quantum wells under different excitation intensities. *Brazilian J. Phys.* 37, 1212–1219. <https://doi.org/10.1590/S0103-97332007000800004>

Milanova, M., Donchev, V., Arnaudov, B., Alonso-Álvarez, D., Terziyska, P., 2020.

GaAsSbN-based p-i-n heterostructures for solar cell applications grown by liquid-phase epitaxy. *J. Mater. Sci. Mater. Electron.* 31, 2073–2080. <https://doi.org/10.1007/s10854-019-02728-5>

Milanova, M., Donchev, V., Kostov, K.L., Alonso-Álvarez, D., Terziyska, P., Avdeev, G.,

Valcheva, E., Kirilov, K., Georgiev, S., 2019. Study of GaAsSb:N bulk layers grown by liquid phase epitaxy for solar cells applications. *Mater. Res. Express* 6, 075521. <https://doi.org/10.1088/2053-1591/ab179f>

Miyashita, N., Ahsan, N., Islam, M.M., Okada, Y., 2012. Study on the device structure of

GaInNAs(Sb) based solar cells for use in 4-junction tandem solar cells, in: *Conference Record of the IEEE Photovoltaic Specialists Conference*. pp. 954–956. <https://doi.org/10.1109/PVSC.2012.6317760>

Miyashita, N., Ahsan, N., Okada, Y., 2013. Effect of antimony on uniform incorporation of

nitrogen atoms in GaInNAs films for solar cell application. *Sol. Energy Mater. Sol. Cells* 111, 127–132. <https://doi.org/10.1016/j.solmat.2012.12.036>

Nunna, K., Iyer, S., Wu, L., Li, J., Bharatan, S., Wei, X., Senger, R.T., Bajaj, K.K., 2007.

Nitrogen incorporation and optical studies of GaAsSbN/GaAs single quantum well heterostructures. *J. Appl. Phys.* 102, 053106. <https://doi.org/10.1063/1.2777448>

Ptak, A.J., France, R., Jiang, C.S., Romero, M.J., 2009. Improved performance of GaInNAs

solar cells grown by molecular-beam epitaxy using increased growth rate instead of

- surfactants. *J. Cryst. Growth* 311, 1876–1880.
<https://doi.org/10.1016/j.jcrysgro.2008.09.184>
- Ptak, A.J., Friedman, D.J., Kurtz, S., Kiehl, J., 2005. Enhanced-depletion-width GaInNAs solar cells grown by molecular-beam epitaxy, in: *Conference Record of the Thirty-First IEEE Photovoltaic Specialists Conference*, 2005. pp. 603–606.
<https://doi.org/10.1109/PVSC.2005.1488203>
- Tan, K.H., Wicaksono, S., Loke, W.K., Li, D., Yoon, S.F., Fitzgerald, E.A., Ringel, S.A., Harris, J.S., 2011. Molecular beam epitaxy grown GaNAsSb 1 eV photovoltaic cell. *J. Cryst. Growth* 335, 66–69. <https://doi.org/10.1016/j.jcrysgro.2011.09.023>
- Thomas, T., Kasamatsu, N., Tan, K.H., Wicaksono, S., Loke, W.K., Yoon, S.F., Johnson, A., Kita, T., Ekins-Daukes, N., 2015. Time-resolved photoluminescence of MBE-grown 1 eV GaAsSbN for multi-junction solar cells, in: *2015 IEEE 42nd Photovoltaic Specialist Conference, PVSC 2015*. Institute of Electrical and Electronics Engineers Inc.
<https://doi.org/10.1109/PVSC.2015.7356069>
- Wiemer, M., Sabnis, V., Yuen, H., 2011. 43.5% efficient lattice matched solar cells, in: *VanSant, K., Sherif, R.A. (Eds.), . p. 810804*. <https://doi.org/10.1117/12.897769>
- Yurong, N.L., Tan, K.H., Loke, W.K., Wicaksono, S., Li, D., Yoon, S.F., Sharma, P., Milakovich, T., Bulsara, M.T., Fitzgerald, E.A., 2017. Performance of 1 eV GaNAsSb-based photovoltaic cell on Si substrate at different growth temperatures. *Prog. Photovoltaics Res. Appl.* 25, 327–332. <https://doi.org/10.1002/pip.2870>